PROCEEDINGS OF SPIE

SPIEDigitalLibrary.org/conference-proceedings-of-spie

Optically controllable coupling between edge and topological waveguide modes of certain graphene metasurfaces

Yupei Wang, Nicolae Panoiu

Yupei Wang, Nicolae C. Panoiu, "Optically controllable coupling between edge and topological waveguide modes of certain graphene metasurfaces," Proc. SPIE 12130, Metamaterials XIII, 1213004 (24 May 2022); doi: 10.1117/12.2621893

SPIE.

Event: SPIE Photonics Europe, 2022, Strasbourg, France

Optically controllable coupling between edge and topological waveguide modes of certain graphene metasurfaces

Yupei Wang and Nicolae C. Panoiu

Department of Electronic and Electrical Engineering, University College London, Torrington Place, London WC1E 7JE, United Kingdom

ABSTRACT

In this paper, optically controllable and topologically protected plasmon transport is implemented via a topological nanohole plasmonic waveguide coupled to a standard edge mode of a graphene metasurface. By introducing nanoholes with different sizes in the unit cell, one breaks the spatial-inversion symmetry of a graphene metasurface in which the topological waveguide is constructed, leading to the emergence of topologically protected modes located in a nontrivial band-gap. Based on the strong Kerr effect and tunable optical properties of graphene, the coupling between the edge and topological interface modes can be efficiently controlled by optical means provided by an optical pump beam injected in a bulk mode. In particular, by tuning the power inserted in the bulk mode, one can control the difference between the wave-vectors of the topological and edge modes and consequently the optical power coupled in the topological mode. Our results show that when the pump power approaches a specific value, the edge and topological modes become phase-matched and the topological waveguide mode can be efficiently excited. Finally, we demonstrated that the optical coupling is strongly dependent on the group-velocity of the pump mode, a device feature that can be important in practical applications.

Keywords: Topological photonics, graphene metasurfaces, Kerr effect, optically controllable coupling

1. INTRODUCTION

Topologically protected edge states located inside topological band-gaps have been attracting increasing research interest, especially due to their novel and unique optical properties and applications, such as unidirectional propagation and robustness against disorder-induced back-scattering.[1–4] Topological modes can be created inside a nontrivial band-gap by breaking the symmetry feature of symmetry-protected Dirac cones.[1–4] For example, the time-inversion symmetry can be broken via an external static magnetic field,[5,6] or an asymmetric spatial perturbation can be introduced to break the spatial-inversion symmetry of the photonic system.[7,8] In this context, valley-Hall topological photonics has been less systematically studied in two-dimensional (2D) optical system, like graphene,[9,10] and likewise nonlinear optical interaction effects in such photonic systems.[11–14] As a promising 2D material with tunable optical properties and strong optical nonlinearity,[15–18] graphene shows a great potential as a unique platform to implement active photonic nanodevices.

In this work, topological valley plasmon transport is implemented in a graphene nanohole plasmonic waveguide by breaking the spatial-inversion symmetry of the graphene nanohole structure. In this configuration, optically controllable coupling between topological interface mode and trivial edge mode can be effectively realized by tuning the pump power inserted in a bulk mode of the graphene metasurface. In the graphene plasmonic waveguide achieved using nanoholes with different sizes, the breaking of spatial-inversion symmetry can gap out symmetry-protected Dirac cones, which generates a nontrivial frequency band-gap. Consequently, topological valley modes emerge inside this nontrivial band-gap. Since the graphene nanohole metasurface is finite, there are additional trivial edge modes whose dispersion curve crosses that of the topological modes, inside the band-gap. The propagation of trivial edge modes is confined at the waveguide boundaries, and their influence on the topological interface mode propagating along the domain-wall interface can be optically controlled with an optical pump inserted in a bulk mode. Employing the strong Kerr effect and tunable optical response of graphene,[15–18]

Further author information: (Send correspondence to Nicolae C. Panoiu)
Nicolae C. Panoiu: E-mail: n.panoiu@ucl.ac.uk, Telephone: +44(0)20 7679 2819

Metamaterials XIII, edited by Kevin F. MacDonald, Isabelle Staude, Anatoly V. Zayats, Proc. of SPIE
Vol. 12130, 1213004 · © 2022 SPIE · 0277-786X · doi: 10.1117/12.2621893

the effective optical coupling between topological interface mode and trivial edge mode is demonstrated in the proposed structure by controlling the phase mismatch between the two optical modes. This work can find particularly useful applications in the design of active topological integrated photonic circuits.

2. TOPOLOGICAL VALLEY PLASMON TRANSPORT IN GRAPHENE NANOHOLE PLASMONIC WAVEGUIDES

The schematics of the graphene nanohole plasmonic waveguide is shown in Fig. 1. The graphene nanohole waveguide consists of two mirror-symmetric domains, which generates a domain-wall interface oriented along the x-axis, as indicated by the light-blue region of Fig. 1(a). Both graphene metasurfaces consist of the same hexagonal periodic distribution of air nanoholes with different radii perforated in a uniform graphene sheet. The primitive unit cell with two holes of different radii R and r is illustrated in Fig. 1(b). In this configuration, we choose the lattice constant, $a = 500\,\text{nm}$, and the radius of the big nanohole, $R = 140\,\text{nm}$.

By introducing the small nanohole with radius r into the unit cell of the graphene metasurface, the spatial-inversion symmetry of the physical system is broken, and the consequences of this fact are presented in Fig. 2(a). Thus, the band diagram of graphene metasurface determined with ($r \neq 0$) and without ($r = 0$) the small nanohole, is calculated in the first Brillouin zone (FBZ).[16] In the case of $r = 0$, indicated by black lines, the spatial-inversion-symmetry protected Dirac cone shows a Dirac point around 12 THz at the K-symmetry point. When a small nanohole with $r = 70\,\text{nm}$ is introduced into the graphene metasurface, the spatial-inversion symmetry of the graphene structure is broken, and consequently a relatively wide nontrivial band-gap ranging from 10.4 THz to 12.5 THz emerges, as indicated by the red curves in Fig. 2(a). In our analysis, we fix $r = 70\,\text{nm}$ unless otherwise stated.

The projected band diagram of graphene nanohole waveguide with finite 20 unit cells width along the y-axis and periodic boundary conditions along the x-axis is given in Fig. 2(b). The bulk modes fill the green region and the light-yellow region represents the nontrivial band-gap. For our graphene nanohole metasurface, the dispersion curve of the nontrivial topological mode represented by the red curve and the dispersion curve of trivial edge mode shown in blue, cross inside the nontrivial band-gap. In order to investigate the optical properties of the topological mode and trivial edge mode, their field distributions are computed numerically. The topological and edge modes at the frequency of 11.7 THz are indicated in Fig. 2(b) by the symbols E_t and E_e, respectively, and the corresponding field profiles are depicted in Figs. 2(c) and 2(d). The optical field of the topological mode is confined at the domain-wall interface, as per Fig. 2(c), whereas the field distribution of edge mode is localized at the upper boundary of the graphene crystal – see Fig. 2(d). Under certain conditions, which will be investigated in the next section, the two modes can couple efficiently and optical power can be transferred to the topological mode.

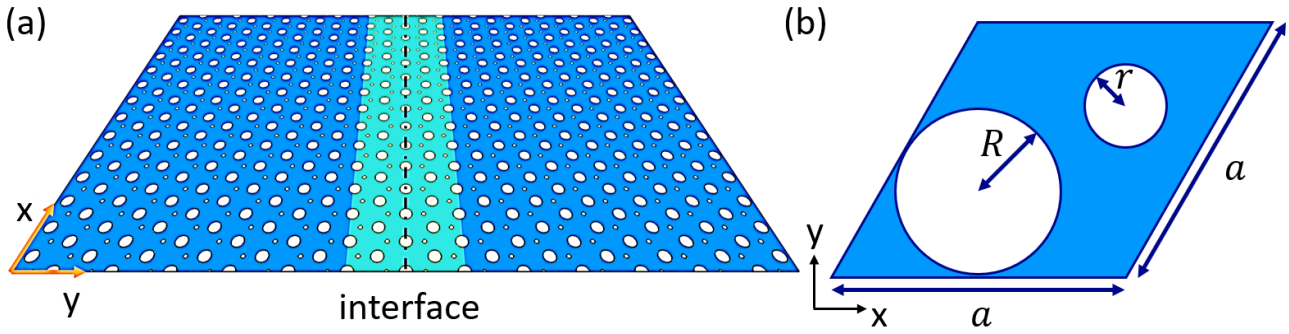

Figure 1. Schematics of a graphene nanohole plasmonic waveguide. (a) Graphene nanohole plasmonic waveguide is composed by left- and right-hand side domains with the same unit cell. The two halves of the graphene nanohole crystal generate a mirror-symmetric domain-wall interface (light blue) oriented along the x-axis. (b) Primitive unit cell of the graphene nanohole plasmonic metasurface containing two etched nanoholes with different radii, R and r. The lattice constant is a.

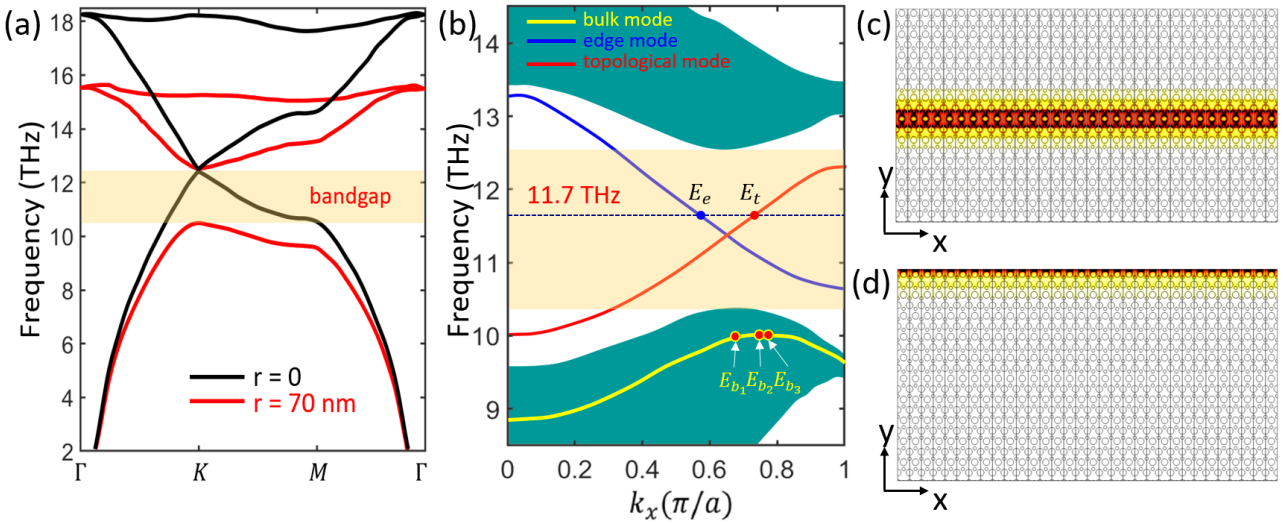

Figure 2. (a) Band diagram of a graphene nanohole crystal without the small nanohole ($r = 0$) and with a nanohole ($r = 70\,\text{nm}$). In the latter case, a nontrivial band-gap marked in yellow emerges. (b) Projected band diagram determined for a finite graphene nanohole plasmonic waveguide, determined when $r = 70\,\text{nm}$. A trivial edge mode (blue line) and a nontrivial topological mode (red line) are formed inside the band-gap. Three bulk modes with different group-velocities are also selected in the bulk region (yellow line). (c) Field profile of the topological mode marked as E_t in (b). (d) Same as in (c), but determined for the edge mode marked as E_e in (b). The frequency of the modes in (c) and (d) is 11.7 THz.

3. OPTICALLY CONTROLLABLE MODE COUPLING

In order to efficiently couple the topological interface mode and trivial edge mode, one can employ the Kerr effect to optically tune the refractive index of the photonic system. Taking advantage of the large second-order nonlinear susceptibility of graphene, the refractive index of the whole system can be significantly modified by optically pumping a bulk mode. These modes have an extended field distribution, and thus can be used effectively to change the refractive index of the graphene metasurface.

When a bulk mode is optically pumped, the projected band diagram of the graphene nanohole waveguide is blue-shifted due to the Kerr effect. This phenomenon is illustrated in Fig. 3(a). When the bulk mode E_{b_1} is used as the pumping mode, the projected band diagram of the graphene waveguide is clearly shifted by around 0.5 THz when the pump power in the bulk mode, P_{b_1}, is increased to $P_{b_1} = 11\,\mu\text{W}$. Moreover, for a given frequency, the wave-vector difference between the topological mode and the edge mode varies with the pump power, which can significantly influence the efficiency of the optical coupling between the two modes. Another physical parameter that can strongly influence the optical coupling between the modes is the group velocity, v_g, of the chosen bulk modes [yellow curve of Fig. 2(b)]. The dispersion of the group-velocity of the bulk mode, as well as that of the group index, $n_g = c/v_g$, are presented are given in Fig. 3(b). It can be seen from this figure that from point E_{b_1} to point E_{b_3}, the group velocity steeply decreases approaching zero, and the group index rapidly grows over 1000 in this same frequency interval. Note that for such large values of the group index the device operates in the slow-light (SL) regime.

Since the wave-vector difference between the topological mode and edge mode varies with the pump power, the coupling between these modes, and consequently the amount of power that can be coupled in the topological mode, can be controlled optically. The power injected in the bulk modes E_{b_1}, E_{b_2}, and E_{b_3} results in an increase of the refractive index of graphene nanohole waveguide due to the strong Kerr effect of graphene. Therefore, if a dipole source with frequency 11.7 THz is placed near the upper boundary of the metasurface so as to excite the trivial edge mode, the optical pump can be used to control the amount of power that couples in the topological mode.

The optically controllable coupling between edge and topological modes without and with pump power injected in the E_{b_1} bulk mode are indicated in Fig. 4(a) and 4(b), respectively. From the projected band

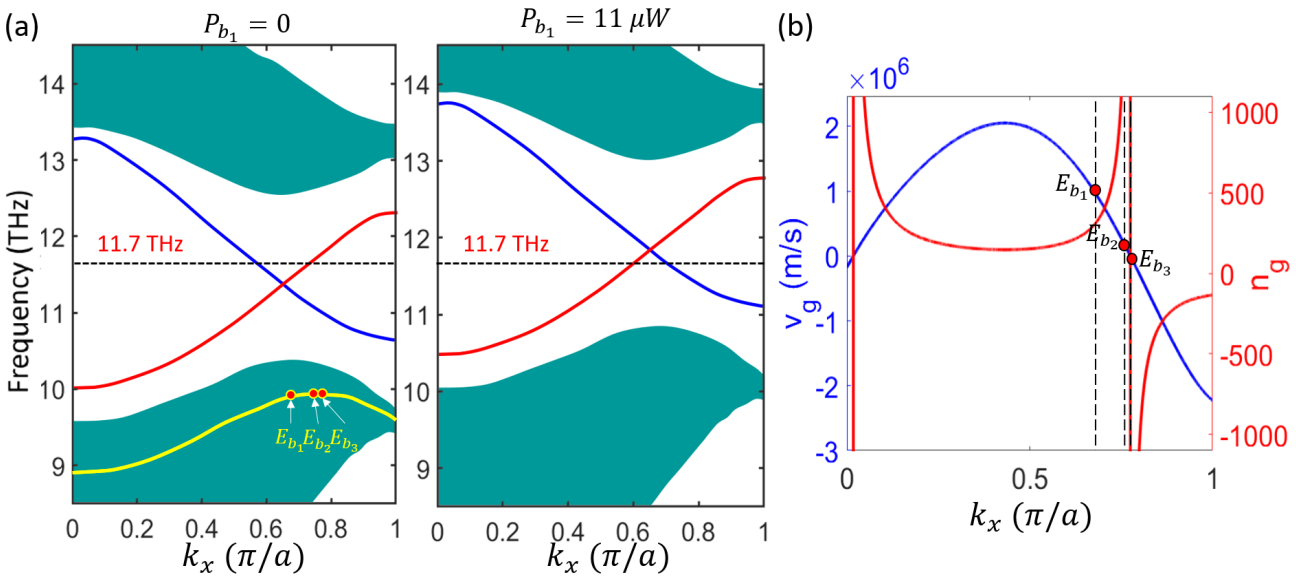

Figure 3. (a) Projected band diagram of graphene nanohole plasmonic waveguide when the bulk mode E_{b_1} is optically pumped with a pump power of $P_{b_1} = 0$ and $P_{b_1} = 11\,\mu$W, respectively. (b) Variation of group-velocity v_g (left axis) and group-index n_g (right axis) determined for the bulk mode marked in yellow in Fig. 2(b).

diagram corresponding to $P_{b_1} = 0$ in Fig. 3(a), when the trivial edge mode is excited at 11.7 THz, the wave-vector difference between edge mode and topological mode is relatively large (0.28). As a result, there is a weak coupling between the two modes, a fact illustrated by the field distribution in Fig. 4(a). In particular, one can see in this figure that practically only the trivial edge mode propagates along the upper boundary. However, the wave-vector between edge and topological mode can be reduced to 0.06 when the pump power reaches −20 dBm. Consequently, the edge mode and topological mode can be much more efficiently coupled in this case, a fact demonstrated by the field profile shown in Fig. 4(b). This is illustrated by the fact that a large amount of light is transferred to the topological interface mode and propagates along the x-axis of the domain-wall interface.

To further investigate the mode coupling, we determined the power dependence of the wave-vector difference, Δk, the calculations being performed for different values of v_g. The results of this analysis are summarized in Fig. 4(c). The solid curves represent the wave-vector difference extracted from the projected band diagram whereas dotted curves represent Δk calculated from the Fourier transform of the corresponding propagating fields. The wave-vector differences determined using these methods show the same trend but with a small horizontal shift. Specifically, the wave-vector difference vanishes when the pump power approaches a certain value, for which the two modes can be efficiently coupled, as indicated in Fig. 4(b). When the pump power is injected in the bulk modes E_{b_1}, E_{b_2}, and E_{b_3}, which have different group-velocities, the corresponding power dependencies of Δk are marked in Fig. 4(c) by red, blue, and black curves, respectively. The power corresponding to the case of the (slow-light) mode E_{b_3} for which the phase-matching condition is fulfilled is the smallest among the three cases because in this case v_g of the bulk mode is the smallest.

The transmission η of topological mode, defined as the ratio between the output power of topological mode and the input power of edge mode, can be used to quantify the coupling efficiency between the modes. The power dependence of this physical quantity is given in Fig. 4(d). The dots show simulated results, and the solid curves represent fitted polynomials of 8th-degree. As expected, the transmission of topological mode reaches a maximum value of 0.052 when the pump power approaches the value at which $\Delta k = 0$. Importantly, the closer the pump mode is to the SL region, the lower power is needed to achieve a maximum power transfer.

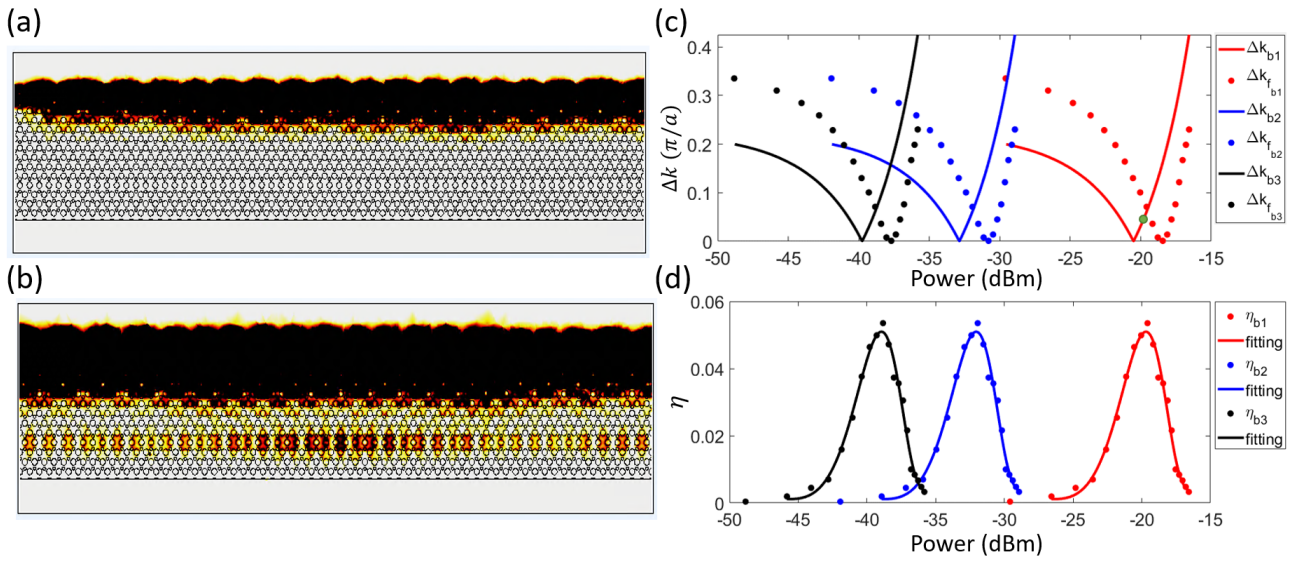

Figure 4. (a) Weak coupling between the edge and topological modes can be achieved for $P = 0$. (b) Strong coupling between the modes is achieved when the pump power injected by bulk mode E_{b_1} is $P_{b_1} = 10\,\mu$W. (c) Dependence of the wave-vector mismatch on the pump power, determined for pump modes E_{b_1} (red), E_{b_2} (blue), and E_{b_3} (black) with different group velocities. Solid lines correspond to the wave-vector difference calculated from the projected band diagram, and dotted curves correspond to the wave-vector difference calculated from the Fourier transform of the electric fields of the topological and edge modes. Green dot represents the wave-vector difference corresponding to the pump power $P_{b_1} = 11\,\mu$W in Fig. 3(a). (d) Power dependence of the transmission of the topological mode, determined for three pump modes with group velocities approaching the SL regime.

4. CONCLUSION

By considering topologically protected plasmon transport in a nanohole plasmonic waveguide implemented in a graphene metasurface, optically controllable coupling between a trivial edge mode and a topological interface mode is studied. The results show that the coupling strength between the modes can be optically controlled via a pump beam injected in a bulk mode. The breaking of spatial-inversion symmetry of a graphene nanohole waveguide leads to the formation of topologically protected interface mode in a nontrivial band-gap. Since the dispersion curves of the edge and topological modes cross inside the band-gap, the two modes can be efficiently coupled by tuning the pump power. When a dipole source is placed at the boundary of the metasurface so as to excite the edge mode, the wave-vector difference between the topological and edge modes varies with the pump power, so that their optical coupling can be conveniently tuned. Our results show that the wave-vector difference can be reduced to zero, and consequently, optical power can be efficiently transferred to the topological mode. When the device is operated in the slow-light regime, a much smaller amount of power is needed to reach the optimum coupling regime.

ACKNOWLEDGMENTS

This work has been supported by the European Research Council (ERC) (ERC-2014-CoG-648328), China Scholarship Council (CSC), and University College London (UCL).

REFERENCES

[1] Lu, L., Joannopoulos, J. D., and Soljacic, "Topological photonics," *Nat. Photonics* **8**, 821 (2014).
[2] Khanikaev, A. B. and Shvets, G., "Two-dimensional topological photonics," *Nat. Photonics* **11**, 763 (2017).
[3] Wu, Y., Li, C., Hu, X., Ao, Y., Zhao, Y., and Gong, Q., "Applications of topological photonics in integrated photonic devices," *Adv. Opt. Mater.* **5**, 1700357 (2017).

[4] Ozawa, T., Price, H. M., Amo, A., Goldman, N., Hafezi, M., Lu, L., Rechtsman, M. C., Schuster, D., Simon, J., Zilberberg, O., and Carusotto, I., "Topological photonics," *Rev. Mod. Phys.* **91**, 015006 (2019).

[5] Haldane, F. D. M., and Raghu, S., "Possible realization of directional optical waveguides in photonic crystals with broken time-reversal symmetry," *Phys. Rev. Lett.* **100**, 013904 (2008).

[6] Poo, Y., Wu, R. X., Lin, Z., Yang, Y., and Chan, C. T., "Experimental realization of self-guiding unidirectional electromagnetic edge states," *Phys. Rev. Lett.* **106**, 093903 (2011).

[7] He, X. T., Liang, E. T., Yuan, J. J., Qiu, H. Y., Chen, X. D., Zhao, F. L., and Dong, J. W., "A silicon-on-insulator slab for topological valley transport," *Nat. Commun.* **10**, 1-9 (2019).

[8] Shalaev, M. I., Walasik, W., Tsukernik, A., Xu, Y., and Litchinitser, N. M., "Robust topologically protected transport in photonic crystals at telecommunication wavelengths," *Nat. Nanotechnol.* **14**, 31-34 (2019).

[9] Xiao, D., Yao, W., and Niu, Q., "Valley-contrasting physics in graphene: magnetic moment and topological transport," *Phys. Rev. Lett.* **99**, 236809 (2007).

[10] You, J. W., Lan, Z., Bao, Q., and Panoiu, N. C., "Valley-Hall topological plasmons in a graphene nanohole plasmonic crystal waveguide," *IEEE J. Sel. Top. Quantum Electron.* **26**, 1-8 (2020).

[11] Lumer, Y., Plotnik, Y., Rechtsman, M. C., and Segev, M., "Self-localized states in photonic topological insulators," *Phys. Rev. Lett.* **111**, 243905 (2013).

[12] Lan, Z., You, J. W., and Panoiu, N. C., "Nonlinear one-way edge-mode interactions for frequency mixing in topological photonic crystals," *Phys. Rev. B.* **101**, 155422 (2020).

[13] Lan, Z., You, J. W., Ren, Q., Wei, E. I., and Panoiu, N. C., "Second-harmonic generation via double topological valley-Hall kink modes in all-dielectric photonic crystals," *Phys. Rev. A.* **103**, L041502 (2021).

[14] You, J. W., Lan, Z., and Panoiu, N. C., "Four-wave mixing of topological edge plasmons in graphene metasurfaces," *Sci. Adv.* **13**, eaaz3910 (2020).

[15] Grigorenko, A. N., Polini, M., and Novoselov, K. S., "Graphene plasmonics," *Nat. Photonics* **6**, 749-758 (2012).

[16] Wang, Y., You, J. W., Lan, Z., and Panoiu, N. C., "Topological valley plasmon transport in bilayer graphene metasurfaces for sensing applications," *Opt. Lett.* **45**, 3151-3154 (2020).

[17] Dremetsika, E., *et al.* "Measuring the nonlinear refractive index of graphene using the optical Kerr effect method," *Opt. Lett.* **41**, 3281-3284 (2016).

[18] You, J. W. and Panoiu, N. C., "Tunable and dual-broadband giant enhancement of second-harmonic and third-harmonic generation in an optimized graphene-insulator-graphene metasurface," *Phys. Rev. B.* **102**, 121403 (2020).